CELL CYCLE
2022, VOL. 21, NO. 17, 1867–1878
https://doi.org/10.1080/15384101.2022.2074740

Taylor & Francis
Taylor & Francis Group

RESEARCH PAPER

Knockout of cyclin B1 in granulosa cells causes female subfertility

Jinmei Cheng[a,b] and Yixun Liu[b]

[a]School of Medicine, Institute of Reproductive Medicine, Nantong University, Nantong, Jiangsu, China; [b]State Key Laboratory of Stem Cell and Reproductive Biology, Institute of Zoology, Chinese Academy of Sciences, Beijing, Xicheng, China

ABSTRACT

In mammalian cells, cyclin B1 plays a pivotal role in mitotic and meiotic progression. It has been reported that infertility occurs after disruption of *cyclin B1* (*Ccnb1*) in male germ cells and oocytes. However, it remains to be elucidated whether the specific disruption of *Ccnb1* in granulosa cells influences the reproductive activity of female mice. Amhr2 is expressed in granulosa cells (GCs) of the ovary. Here, we mated $Ccnb1^{Flox/Flox}$ mice with a transgenic mouse strain expressing *Amhr2-Cre* to generate GC-specific *Ccnb1* knockout mice. The results showed that $Ccnb1^{Flox/Flox}$, *Amhr2-Cre* (*Ccnb1* cKO) mice were subfertile but had normal oocyte meiotic progress, spindle shape and protein levels of cohesin subunits REC8 and SMC3 on arm chromosomes during meiosis I. A further study found that 32.4% of oocytes from *Ccnb1* cKO mice exhibited chromosome condensation and spindle disassembly after the first polar body extrusion and failed to undergo second meiosis, which was never found in oocytes from $Ccnb1^{Flox/Flox}$ mice. In addition, the percentages of 2-cell embryos, morulas, and blastocysts in the *Ccnb1* mutant group were all dramatically decreased compared to those in the $Ccnb1^{Flox/Flox}$ group (39.2% *vs*. 86.8%, 26.0% *vs*. 85.0%, 19.1% *vs*. 85.8%, respectively). Therefore, GC-specific *Ccnb1* deletion in mice could cause fewer and poor-quality blastocysts and subsequent subfertility, which plays an important role in understanding the function of cyclin B1 in reproduction.

ARTICLE HISTORY
Received 13 August 2021
Revised 26 April 2022
Accepted 3 May 2022

KEYWORDS
Granulosa cells; cyclin B1; oocytes; subfertility

Introduction

In mammalian cells, cyclin B and cyclin-dependent kinase 1 (CDK1) are maturation-promoting factors (MPFs) that govern M-phase entry [1,2]. The activation of MPF requires the dephosphorylation of CDK1 and a sufficient accumulation of Cyclin B [3,4]. Cyclin B has three types: Cyclin B1, Cyclin B2, and Cyclin B3. Cyclin B3 collaborates with CDK2. The association of Cyclin B1 and Cyclin B2 with CDK1 promotes CDK1 activation in mammalian cells [4,5]. Cyclin B1-Cdk1 is inactive in G2 phase and activated at a set time before nuclear envelope breakdown [6]. Therefore, the activation of cyclin B-Cdk1 is generally considered to trigger entry into mitosis [7]. In addition, *Ccnb1-null* embryos die, whereas *Ccnb2-null* mice develop normally and do not display any obvious abnormalities [8]. Further study found that embryos arrest at the four-cell stage without Cyclin B1, and Cyclin B2 does not make an apparent contribution to early cell divisions [9]. These results imply that cyclin B1 is critically required for mouse embryogenesis, whereas cyclin B2 is dispensable for mouse embryonic development. In males, the ablation of cyclin B1 in germ cells did not influence the meiosis of spermatocytes and fertility, but cyclin B1 is critically required for the proliferation of gonocytes and spermatogonia [10]. In females, the synthesis and degradation of Cyclin B1 regulate the timing of meiotic progression [5]. Recently, Li *et al*. showed that mouse oocytes undergo germinal vesicle breakdown (GVBD) and polar body 1 extrusion (PBE) but fail to arrest at metaphase (MII) *in vivo* deletion of cyclin B1 [11].

Furthermore, Cyclin B1-mediated inhibition of excess separase is required for cleaving the cohesin subunit Rec8 protein to induce timely chromosome disjunction [12–14]. Andrew *et al*. indicated that Cyclin B1 binding, rather than phosphorylation, is the key inhibitory separase activity [15]. A recent study showed that cyclin B2/CDK1 is also

CONTACT Yixun Liu liuyx@ioz.ac.cn School of Medicine, Institute of Reproductive Medicine, Nantong University, Nantong 226001, China; Jinmei Cheng chengjinmeixdg@163.com State Key Laboratory of Stem Cell and Reproductive Biology, Institute of Zoology, Chinese Academy of Sciences, Beijing 100101, China

responsible for separase inhibition via inhibitory phosphorylation to regulate chromosome separation in oocyte meiosis [16]. In brief, cyclin B has a key role in oocyte chromosome segregation.

Ovarian granulosa cells provide oocytes with indispensable signals and metabolites required for oocyte growth and maturation by gap junctions [17]. Granulosa cells play a crucial role in oocyte development. It has been reported that lacking the *Ccnb1* gene in male germ cells causes germ cell depletion and subsequent infertility. A recent study indicated that the deletion of *Ccnb1* in oocytes caused sterility in female mice. However, it remains unknown whether specific disruption of *Ccnb1* in granulosa cells influences the reproductive activity of female mice. To clarify this problem, we mated *Ccnb1* $^{Flox/Flox}$ mice with a transgenic mouse strain expressing *Amhr2-Cre*, which is expressed in granulosa cells of the ovary [18,19]. Our results demonstrated that conditional knockout female mice are subfertile because of poor embryonic development, which is important for understanding the function of cyclin B1 in the reproductive system.

Materials and methods

All experimental protocols and animal handling procedures were conducted in accordance with the guidelines and procedures approved by the Institutional Animal Care and Use Committee of Nantong University and the Institutional Animal Care and Use Committee at the Institute of Zoology (IOZ), Chinese Academy of Sciences (CAS). All chemicals and drugs were purchased from Sigma (St. Louis, MO, USA), unless otherwise indicated.

Mice

The *Ccnb1*$^{Flox/Flox}$ and *Ccnb1* $^{Flox/Flox}$, *Amhr2-Cre* (*Ccnb1* cKO) mice were generated as described previously [11,18]. Briefly, an embryonic stem cell line (clone EPD0357_2_A11) with the *Ccnb1* gene was microinjected into the embryo to generate *Ccnb1*$^{Flox/Flox}$ mice. The *Ccnb1* cKO mice were obtained by crossing *Ccnb1*$^{Flox/Flox}$ mice with transgenic mice carrying *Amhr2* promoter–mediated *Cre* recombinase. Genotypes were identified by polymerase chain reaction (PCR) analysis, as previously reported [10,18]. The bands of Ccnb1 $^{Flox/+}$, *Ccnb1* cKO are shown in Figure 1b. All mice were maintained in a C57BL/6;129/SvEv mixed background and were housed in a controlled environment (12 h light/dark cycle, 22 ± 1°C, 60%–70% humidity) and fed ad libitum with standard chow.

Fertility rate

Six- to 8-wk-old *Ccnb1*$^{Flox/Flox}$ (n = 7) and *Ccnb1* cKO mice (n = 7) were separately mated with wild-type C57BL/6 males for 6 months in a 1:2 ratio. Litter sizes were assessed after birth.

Superovulation, oocyte and embryo collection and culture

Superovulation was performed in *Ccnb1*$^{Flox/Flox}$ and *Ccnb1* cKO mice. Briefly, mice received a single intraperitoneal injection of 10 IU of eCG per mouse (Ningbo Hormone Product Co. Ningbo) followed 48 hrs later by 10 IU hCG (Ningbo Hormone Product Co.) and were immediately mated with wild-type C57BL/6 males. Zygotes were collected from the ampullar region of the oviduct when a vaginal plug was found the following day and cultured in the KSOM. Embryos at the two-cell, morula and blastocyst stages were examined and recorded at 24, 48 and 96 hrs after the start of culturing, respectively.

To collect full-grown germinal vesicle (GV) oocytes, the mice were sacrificed by cervical dislocation 48 hrs after intraperitoneal injection of 5 IU of eCG. Full-grown GV oocytes were released by puncturing ovaries with a 28-gauge microinjection needle and then collected by mouth pipette in M2 medium supplemented with 100 mM dbcAMP. Cumulus cells were subsequently removed by repeated pipetting through a narrow-bore pipette. The GV oocytes were matured in M16 medium for 7.5–8 hrs to collect metaphase I (MI). The culture process took place in an incubator at 37°C with 5% CO_2 in the air.

Granulosa cell isolation

Isolation of granulosa cells was performed as described previously [20,21]. Briefly, immature female mice (3-wk-old) were injected with 5 IU

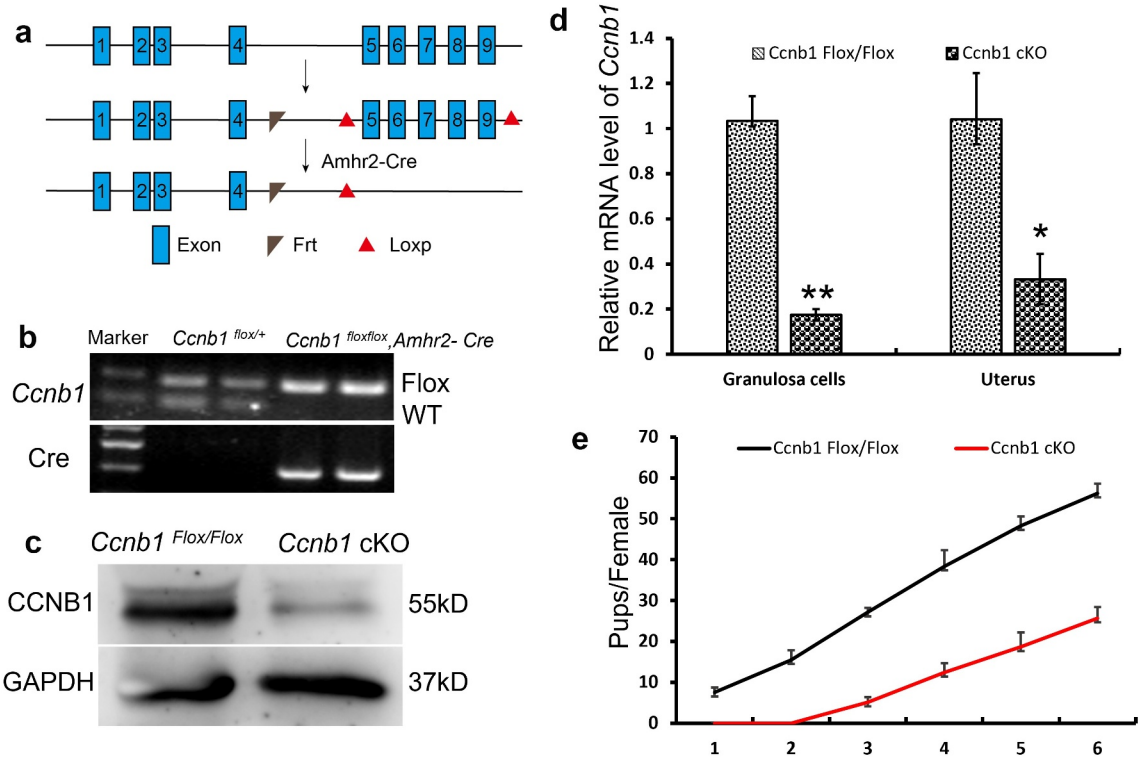

Figure 1. Subfertility of *Ccnb1* cKO female mice. (a) Generation of *Ccnb1* cKO mice. Exons 5–9 of *Ccnb1* were deleted by *Amhr2-Cre*–mediated recombination. (b) Genotyping PCR for the identification of the *Ccnb1* $^{Flox/+}$ and *Ccnb1* cKO mice. (c) Western blot demonstrating the significant decrease in cyclin B1 protein in knockout mouse GCs. The GCs of each lane were collected from one mouse, and the level of GAPDH was used as an internal control. (d) qRT–PCR analysis showing the conditional reduction of *Ccnb1* mRNA in granulosa cells and uterine extracts. The data are expressed as the mean ± SEM. *$P < 0.05$, **$P < 0.01$. (e) Comparison of the accumulative number of pups per *Ccnb1* $^{Flox/Flox}$ *and Ccnb1* cKO females (n = 6 for each group). Each experiment was repeated a minimum of three times.

of eCG, and 46–48 h later, large antral follicles were punctured with needles, and granulosa cells were collected into M2 medium. After filtration through a nylon mesh with a 40-μm pore size, the granulosa cells were recovered and subjected to RNA isolation and protein extraction.

MI oocyte chromosome spread and immunofluorescence

Oocyte chromosome spreads and immunofluorescence were conducted according to a previous report with modifications [22,23]. Briefly, the zona pellucid of oocytes was removed prior to fixation by brief exposure to acid Tyrode's solution. Zona-free oocytes were mounted on glass slides and fixed in a solution of 1% paraformaldehyde (PFA) in distilled H_2O (pH 9.2) containing 0.15% Triton X-100 and 3 mM dithiothreitol. The slides were left to dry and then blocked with 1% bovine serum albumin (BSA) in PBS for 1 h at room temperature. The slides were incubated with Rec8 polyclonal antibody (1:50, 10,793-1-AP, Proteintech), human anti-centromere autoimmune serum (1:100, HCT-010, Immunovision) and Smc3 monoclonal antibody (1:20; ab128919, Abcam) diluted in blocking solution at 37°C for 1 h. After brief washes with PBS containing 0.03% BSA and 0.01% Triton X-100, the slides were then incubated with secondary antibodies for 1 h at 37°C. Following DNA staining with DAPI, the slides were mounted on glass coverslips and examined with a laser scanning confocal microscope (Zeiss LSM 780 META, Germany).

To assess the quality of blastocysts, blastocysts were fixed in a solution of 2% PFA in PBS for 30 min at room temperature and then permeated in 0.2% Triton X-100 for 20 mins. After blocking in PBS with 1% BSA for 20 min, blastocysts were incubated with anti-cleaved Caspase 3 (1:50, D175, Cell

Signaling) at 37°C for 1 h. An anti-rabbit FITC secondary antibody was used to stain these blastocysts for 1 h at 37°C. After DAPI staining for 10 mins, blastocysts were mounted on glass slides and examined with a confocal laser scanning microscope (Zeiss LSM 780 META, Germany).

Time-lapse confocal microscopy of live oocytes

Hoechst 3342 and SiR-Tubulin (Cytoskeleton, CY-SC002) were used to image DNA and tubulin in living oocytes, respectively. For time-lapse imaging, oocytes were housed in an air-controlled environment at 37°C and 5% CO_2. Images were captured every 30 mins with a z-resolution of 2.0 mm. Tracking lasted for 16–17 hrs using the PerkinElmer Ultra-View-Vox 20 X (NA 1.4) objective on a spinning disk confocal microscope equipped with 532-nm and 405-nm excitation lasers. To assess the kinetics of GVBD and PBE, the maturation process of the whole oocyte was also tracked by this system with transparent light.

Hematoxylin and eosin (H&E)

The ovaries of 8-wk-old *Ccnb1*$^{Flox/Flox}$ and *Ccnb1* cKO mice were isolated, fixed with 4% PFA, stored in 70% ethanol and embedded in paraffin. Tissue sections (5 μm thick) were cut and mounted on glass slides. These slides were deparaffinized, rehydrated, and then stained with H&E. Ovarian primordial follicles and activated follicles were counted in all the sections of one ovary. Quantification of ovarian follicles was performed as previously reported [22,24]. Only follicles with an oocyte nucleus in the section were counted.

Western blotting

Western blotting experiments were conducted as previously reported [18]. Briefly, the proteins were extracted from granulosa cells by radioimmunoprecipitation assay lysis buffer. The proteins were electrophoresed in 10% SDS–PAGE gels and transferred to polyvinylidene fluoride (PVDF) membranes. The membranes were blocked in 5% milk for 1 h at room temperature (RT) and then incubated overnight at 4°C with anti-Cyclin B1 (1:400, mouse, Abcam) and anti-GAPDH (1:5000, mouse, MB001, Bioworld) antibodies. After washing three times, the membranes were incubated with an HRP-conjugated goat anti-mouse antibody (ZSGB-BIO) for 1–2 h at RT. Finally, the membranes were scanned using an enhanced chemiluminescent detection system. The protein level was normalized to the GAPDH abundance.

RT–PCR and qRT–PCR analysis

Total RNA was extracted from granulosa cells and the uterus using TRIzol. An M-MLV Reverse Transcriptase kit (Promega, CA) was used for reverse transcription of RNA samples. Real-time quantitative PCR was performed with GoTaq qPCR Master Mix (A6001/2; Promega) according to the manufacturer's protocols. Sample cycle threshold (Ct) values were normalized to *Gapdh* Ct values, and relative expression levels were calculated using the $2^{-\Delta\Delta Ct}$ method. For genotyping, mouse tail fractions were excised and lysed as templates, and then, PCR was performed using Master Mix (TSI NGKE) according to the manufacturer's protocols. Primers for quantitative RT–PCR were as follows: *Gapdh* forward, 5' AGGTCGGTGTGAACGGAT-3', and reverse, 5'- TGTAGACCATGTAGTTGA-3'; *Ccnb1* forward, 5'-GAG CTA TCC TCA TTG ACT GG-3', and reverse, 5'-CAT CTT CTT GGGCAC ACA AC-3'; and *Ccnb2* forward, 5'-GCC AAG AGC CAT GTG ACTATC-3', and reverse, 5'-CAG AGC TGG TAC TTT GGT GTTC-3'. Primers for RT–PCR: *Ccnb1* forward, 5'- CAA GCACTT TAC CAC CGA ACT AT-3', and reverse, 5'-GTC AGA AGA CAGCTA CTG TGT AC-3'; *Amhr2-Cre* forward, TTCAATTTACTGACCGTACACC, and reverse, CGTTTTCTTTTCGGATCC.

Statistical analysis

All experiments were repeated at least 3 times. The data in the present study were analyzed using Student's t-test in SPSS (Statistical Package for the Social Sciences) 19.0 software (SPSS, Inc., Chicago, IL, USA). $P < 0.05$ and $P < 0.01$ values were considered statistically significant. Images were analyzed with ImageJ software (National Institutes of Health).

Results

GC-specific cyclin B1 knockout leads to female subfertility

The *Amhr2- Cre* mouse has been used extensively as a means to target deletion in granulosa cells [20,25–27]. To delete Cyclin B1 in GCs, we generated *Ccnb1* cKO mice, as shown in Figure 1a. CRE-mediated excision of the regions between exons 5 and 9 of the *Ccnb1* gene converted the floxed allele into a recombined allele no longer capable of encoding a functional cyclin B1 protein [11]. We identified the genotypes of *Ccnb1* $^{Flox/Flox}$ and *Amhr2-Cre* mice by PCR (Figure 1b). Using Western blotting and qPCR, we confirmed the significant decrease in Cyclin B1 protein and mRNA from *Ccnb1* cKO mouse GCs (Figure 1c,d, $p < 0.01$). Incomplete ablation of mRNA transcripts and proteins in *Ccnb1* cKO mouse GCs was potentially caused by the variable efficiency of Cre recombinase, which has been observed in studies using *Amhr2-Cre* [20,21,28,29].

Amhr2-Cre is also present in the muscular layer of the uterus [19]. Therefore, the conditional knockout efficiency in *Ccnb1* cKO mice was also confirmed by a significant decrease in *Ccnb1* mRNA levels in their uteri (Figure 1d, $p < 0.05$). However, the morphology of the oviduct and uterus were normal (data not shown). After mating for > 6 months, we found that the *Ccnb1* cKO female mice were subfertile (Figure 1e).

Normal follicular development and oocyte meiosis in CcnB1 mutant females

To explore the reason for subfertility in GC-specific Cyclin B1 knockout mice, we investigated their follicular development using **H&E** staining. As shown in Figure 2a and Figure S1, ovarian morphology and the number of primordial and activated follicles were not significantly different between the *Ccnb1* $^{Flox/Flox}$ and *Ccnb1* cKO groups. Furthermore, we found that oocytes in GC-specific Cyclin B1 knockout mice underwent GVBD and PBE with similar efficiencies and kinetics as those in the control mice (Figure 2c,d). Cyclin B2 has been reported to compensate for the loss of Cyclin B1 in *GDF9-Ccnb1*−/− oocytes [30]. Therefore, we detected the level of Cyclin B2 expression in the mouse GCs and uterus using qRT–PCR. As Figure 4b shows, the level of *Ccnb2* mRNA expression was significantly increased in the GCs and uterus of *Ccnb1* cKO mice. Given that the ablation of cyclin B1 in GCs could not affect follicular development and oocyte meiosis, cyclin B2 may compensate for the function of cyclin B1 in mouse GCs.

GC-specific Cyclin B1 deletion did not affect arm chromosome cohesion

Aged oocytes with normal meiosis experience the loss of cohesion [31]. Cyclin B1-mediated inhibition of excess separase is required for timely chromosome disjunction in mouse oocytes [12]. To explore whether GC-specific Cyclin B1 deletion influences arm cohesion in oocytes, the expression of cohesin subunit REC8 and SMC3 proteins on chromosome arms was detected in the MI stage by immunofluorescence (Figure 3a). We found that the relative REC8 and SMC3 fluorescence intensities on chromosome arms were similar between the *Ccnb1*$^{Flox/Flox}$ and *Ccnb1* cKO groups (Figure 3b). In brief, cyclin B1 in GCs is dispensable for the maintenance of arm cohesion in oocyte meiosis I.

Oocyte meiotic progress was not affected by GC-specific Cyclin B1 deletion

The synthesis and degradation of cyclin B1 regulate the timing of meiotic progression, especially GV arrest/GV breakdown and metaphase/anaphase transition of the first meiosis in oocyte maturation [4]. To explore whether GC-specific Cyclin B1 deletion impacts oocyte meiotic progression, we examined the timeframes from GVBD to congression and from congression to anaphase by chromosome change with time-lapse confocal live imaging (Figure 4a,b). The results showed that the GVBD/congression and congression/anaphase transitions of the first meiosis were not significantly different between the *Ccnb1*$^{Flox/Flox}$ and *Ccnb1* cKO groups (Figure 4c). Additionally, the whole time from GVBD to anaphase was also similar between the two groups (Figure 4c). Hence, GC-specific Cyclin B1 deletion does not influence the first meiotic progress of mouse oocytes.

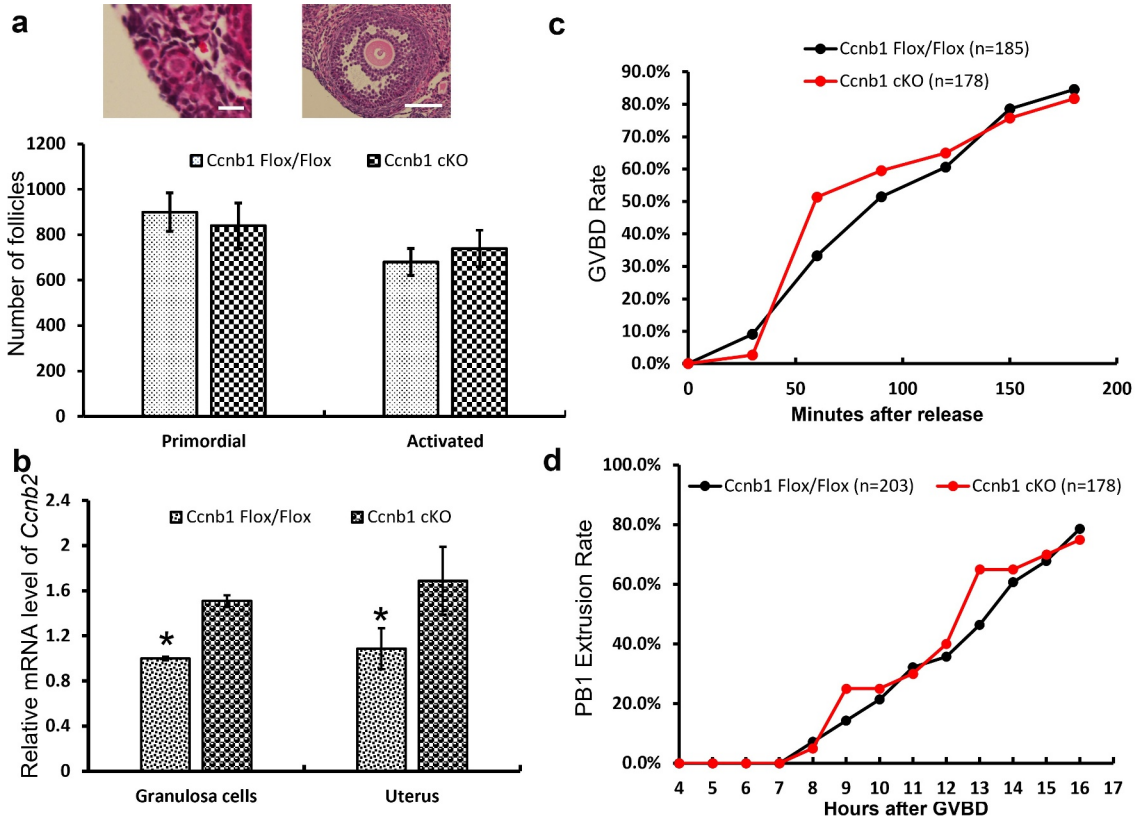

Figure 2. GC-specific Cyclin B1 deletion did not affect follicular development or oocyte meiosis. (a) Representative images of primordial and activated follicles are shown above the bar graph. Left Bar = 5 μm, right bar = 150 μm. The numbers of primordial and activated follicles per ovary were quantified. (b) The level of *Ccnb2* mRNA expression was examined in the GCs and uterus of *Ccnb1* $^{Flox/Flox}$ and *Ccnb1* cKO females. *Gapdh* served as the internal control gene. The data are expressed as the mean ± SEM. *$P < 0.05$. (c) Kinetics of germinal vesicle breakdown (GVBD). GV oocytes were isolated in M2 medium containing dbcAMP, which inhibits GVBD, and were released into inhibitor-free medium (at time = 0). The number of oocytes examined is indicated (n). (d) Kinetics of polar body extrusion (PBE). Oocytes that had undergone GVBD within 4 hrs after release into dbcAMP-free M16 medium were selected (at time = 4). The number of oocytes examined is indicated (n). Error bars denote the means ± SEM of three experiments.

GC-specific Cyclin B1 deletion leads to failing second meiosis of oocytes

Our previous report found that oocyte-specific Cyclin B1 deletion could cause condensed chromosomes after PBE [11]. To further analyze the reason for the subfertility of GC-specific Cyclin B1 deletion mice, we conducted live-cell imaging of oocytes after incubating Hoechst 3342 and Sir-tubulin to label chromosomes and spindles, respectively (Figure 5a, supplemental videos 1 and 2). The dynamics of nuclear changes, spindle assembly, and chromosome segregation were monitored during live-cell imaging. The results showed that the first meiosis of oocytes from wild-type and knockout mice was similar at changes in spindle morphology and chromosome position (Figure 5a). Additionally, the ratio of normal spindle morphology at the metaphase I stage was not significantly different between the two groups (Figure 5c). In the normal group, the oocytes entered the second meiosis after PBE and arrested at the metaphase II stage. The metaphase II stage is characterized by chromosome alignment on the equatorial plane with a normally shaped spindle (Figure 5a). However, we observed that some oocytes in the *Ccnb1* cKO group did not show the typical characteristics of the metaphase II stage. Rather, they showed condensed chromosomes, disassembled spindles and interphase-like nuclei approximately 4 hours after PBE (Figure 5a), which is typically seen in *Ccnb1*-null oocytes [11]. In other words, these oocytes were unable to enter the second meiosis and were arrested at interphase. This was observed in 32.4% of the knockout oocytes, which was significantly higher than that in the control group (Figure 5b, $p < 0.0001$).

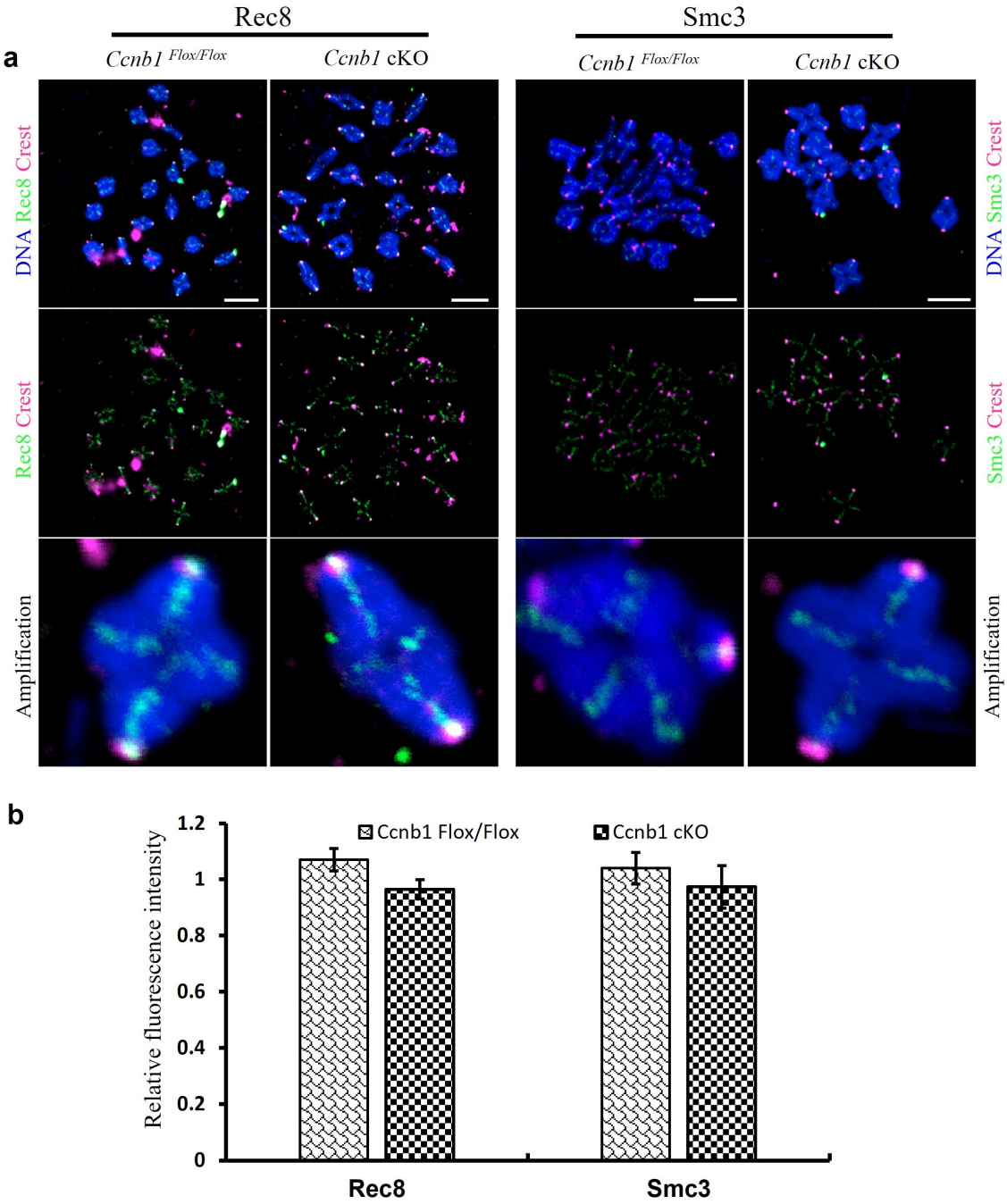

Figure 3. The expression levels of REC8 and SMC3 proteins on arm chromosomes. (a) The levels of chromosome-associated REC8 and SMC3 proteins were detected by immunofluorescence in oocytes at the MI stage. Representative images show DNA (blue), CREST (magenta), REC8 (green) and SMC3 (green). Scale bar, 5 μm. (b) REC8 and SMC3 fluorescence intensities were quantified. Data are the means ± SEM; ≥152 bivalents of each group were analyzed.

Reduced embryonic development and poor quality of blastocysts in GC-specific Cyclin B1 deletion mice

To analyze the ability of fertilization and early embryonic development in GC-specific cyclin B1 knockout females, we crossed *Ccnb1*-mutant and control females with wild-type males. The zygotes were collected and cultured *in vitro*. A total of 32.4% of oocytes from Cyclin B1 knockout mice formed interphase-like nuclei (Figure 5b). Oocytes with interphase nuclei and real zygotes are very difficult to distinguish after collection from the

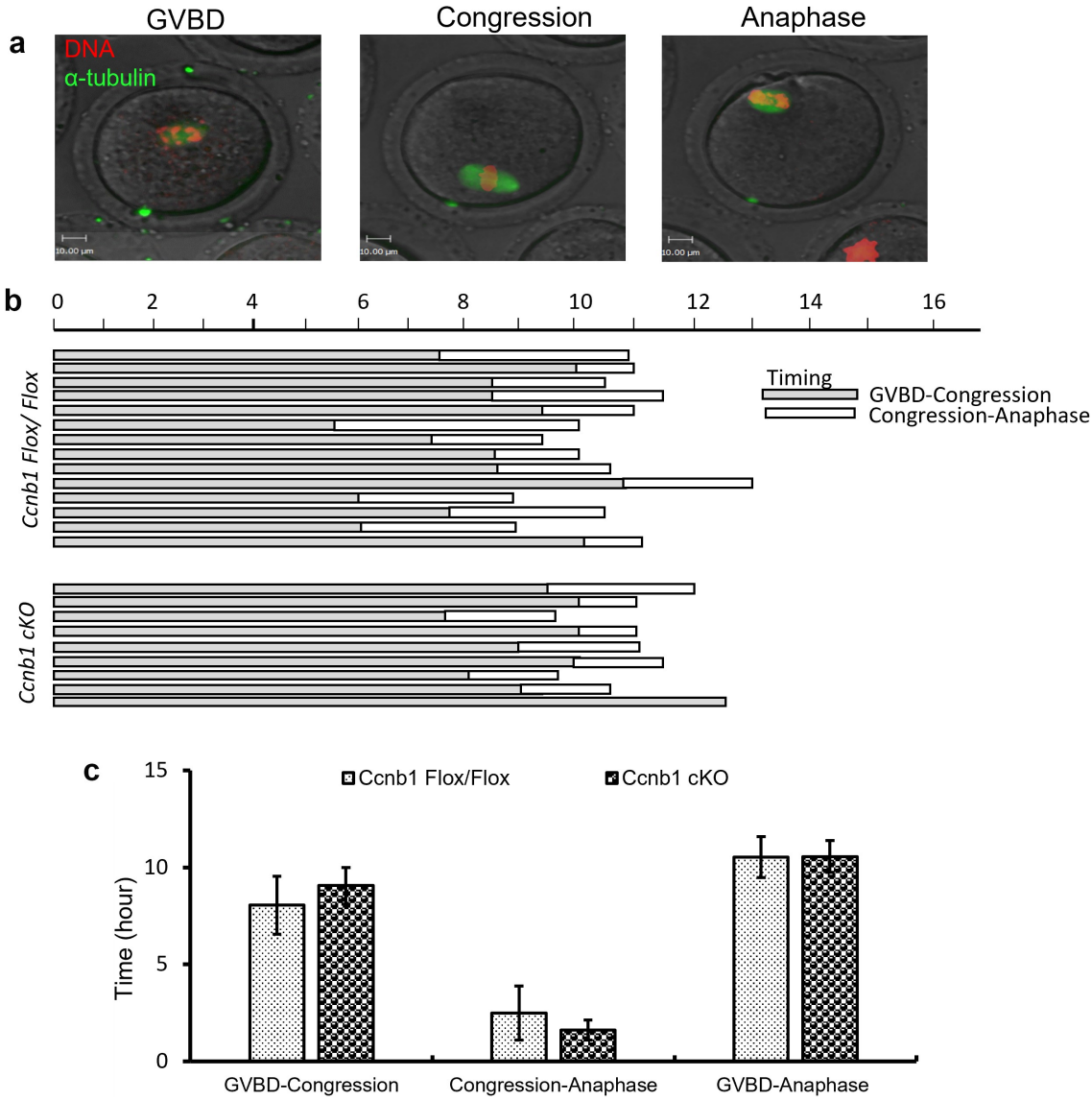

Figure 4. The first meiotic progress of oocytes. (a) Representative images of GVBD, congression and anaphase onset are shown. (b) Timeline shows a similar interval from GVBD to congression (shaded bar) and from congression to anaphase (white bar). Data are based on a subset of oocytes (n = 80 oocytes from *Ccnb1*$^{Flox/Flox}$ mice; n = 93 oocytes from *Ccnb1* cKO mice) in which chromosomes could be tracked during congression and anaphase I onset. (c) The graph shows that there was no significant difference in the intervals from GVBD to congression and from congression to anaphase in oocytes from *Ccnb1*^{Flox}/^{Flox} and *Ccnb1* cKO mice. In each experiment, the data shown represent more than 3 replications. Data are the mean ± SEM.

ampulla of the oviduct. Hence, the results revealed that the oocytes from *Ccnb1* cKO mice were seemingly fertilized successfully (Figure 6a). The rate of zygotes did not seemingly show a significant difference between the two groups by calculating one pronucleus as the standard of zygotes (83.5% ± 0.12 *vs.* 96.0% ± 0.05) (Figure 6a,b), as was the case for *Ccnb1-null* oocytes [11]. However, the rates of 2-cell, morula and blastocyst formation in the Cyclin B1 mutant group were all dramatically decreased compared to those in the *Ccnb1* $^{Flox/Flox}$ group (39.2% ± 0.01 *vs.* 86.8% ± 0.02, 26.0% ± 0.03 *vs.* 85.0% ± 0.01, 19.1% ± 0.01 *vs.* 85.8% ± 0.03, respectively) (Figure 6a,b). The numbers of cell nuclei and cleaved caspase 3 proteins in blastocysts were stained and counted to detect their quality (Figure 6c). A significant decrease in the total cell number (84.7 ± 1.26 *vs.*

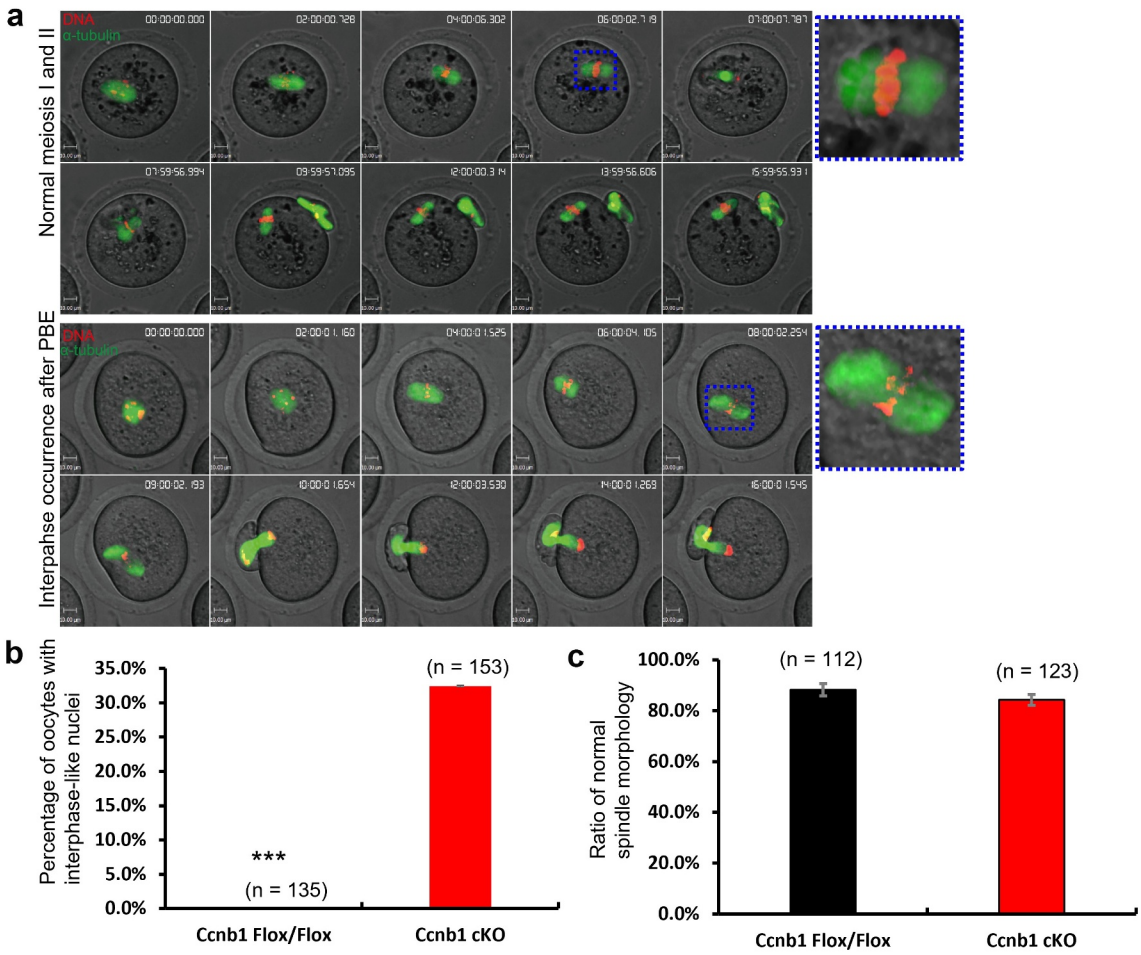

Figure 5. GC-specific Cyclin B1 deletion decreased the rate of second meiosis of oocytes. (a) Chromosomes and spindles were labeled with Hoechst 3342 and Sir-tubulin, respectively. The images were captured at 30-min intervals over 16–17 hrs, and representative images are shown. Movies showing normal first and second meiosis and interphase occurrence after PB1 extrusion are available (Supplemental Videos S1, S2). The spindle morphology in metaphase I is marked with a blue square and magnified on the right side. Scale bar, 10 μm. (b) The percentage of oocytes with interphase-like nuclei was calculated. *** $P < 0.0001$. (c) The ratio of the normal spindle morphology at the metaphase I stage was quantified. Data are the means ± SEM. In B and C, the numbers of analyzed oocytes are indicated above the bars.

39.6 ± 1.21, $P < 0.01$) and a striking increase in the expression of cleaved caspase 3 (0.8 ± 0.08 *vs.* 1.92 ± 0.11, $P < 0.01$) were observed in the *Ccnb1*-mutant group compared with the control group (Figure 6d,e). These results suggest that GC-specific Cyclin B1 deletion could lead to decreased embryonic development and poor blastocyst quality.

Discussion

In mammalian cells, cyclin B1 plays a crucial role in mitosis and meiosis. Cyclin $B1^{-/-}$ embryos arrest in G2 phase after just two divisions [9]. Gonocytes and spermatogonia without Cyclin B1 were unable to proliferate normally, and apoptosis was increased [10]. Oocytes depleted of cyclin B1 could not enter the second meiosis and formed interphase-like nuclei after the first meiosis [11]. In the present study, we used granulosa cell-specific knockout mice to supplement the role of Cyclin B1 in the reproductive activity of female mice. We show that, unlike the role of cyclin B1 in oocytes and embryos, ovaries in GC-specific cyclin B1 deletion mice displayed normal ovarian morphology and follicular development (Figure 2a), suggesting that cyclin B1 is less important for

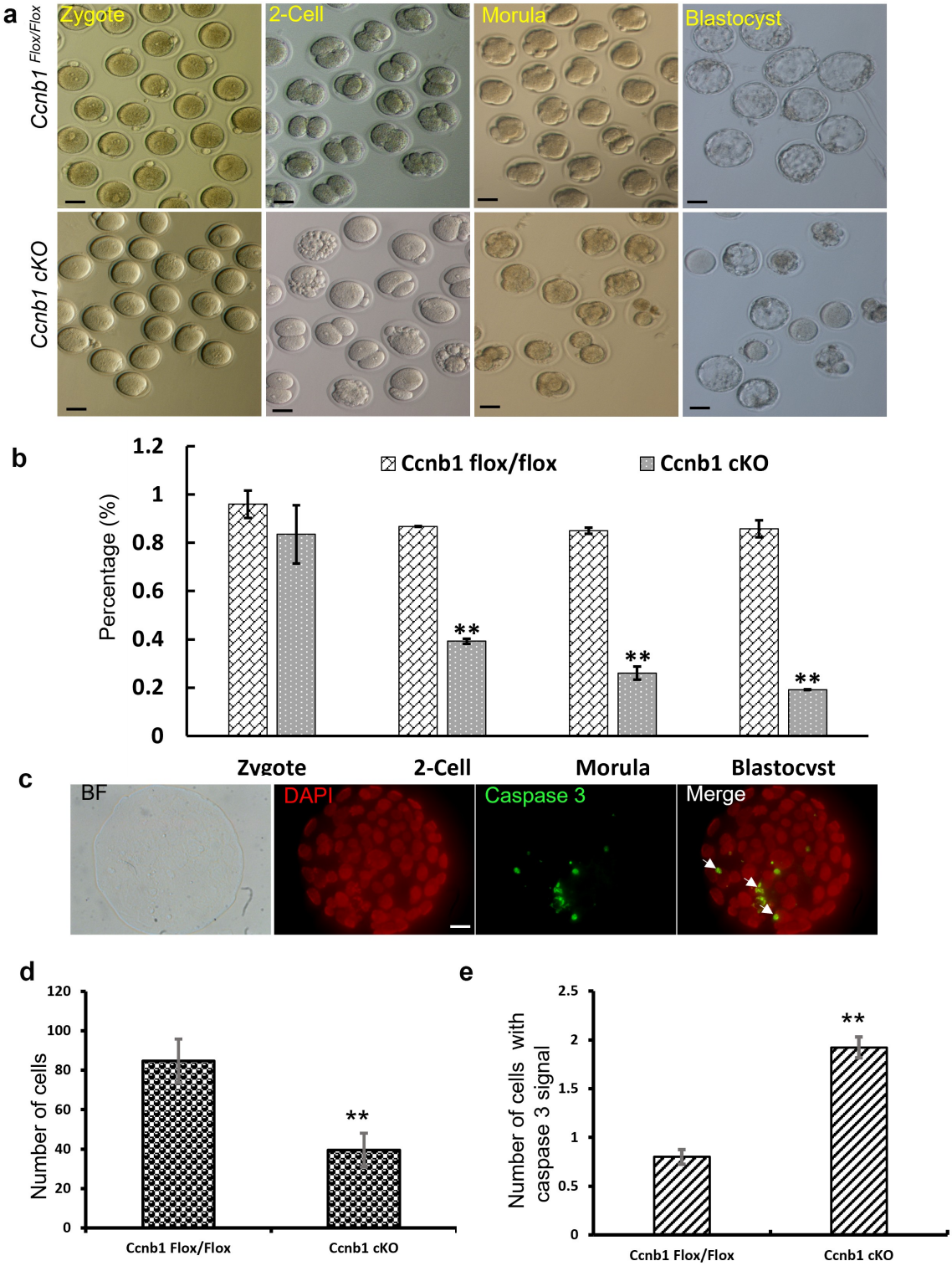

Figure 6. GC-specific Cyclin B1 deletion gave rise to abnormal embryonic development and poor blastocyst quality. (a) Representative images of zygotes, 2-cell embryos, morulas and blastocysts are shown in the *Ccnb1*$^{Flox/Flox}$ and *Ccnb1* cKO groups. Scale bar, 50 μm. (b) The percentages of zygotes, 2-cell embryos, morulas, and blastocysts are shown. (c) The blastocysts were stained with cleaved caspase 3 (*white arrow*, green) and DAPI (red). BF, brightfield. Scale bar, 10 μm. (d) The average cell number of one blastocyst. (e) The number of cells containing cleaved caspase 3 signals in one blastocyst. The data are the means ± SEM. In (B), (D) and (E), ** $P < 0.01$, > 30 oocytes were examined in each experiment. Each experiment was repeated more than 3 times.

granulosa cell proliferation and development. Cyclin B2 could compensate for the absence of Cyclin B1 in mammalian tissue culture cells [32,33]. In mouse oocytes, Cyclin B2 could replace Cyclin B1 to maintain meiotic progress in the first meiosis [11]. Our results found that cyclin B2 mRNA was dramatically increased in mutant GCs and the uterus (Figure 2b). Therefore, Cyclin B2 may compensate for the absence of Cyclin B1 in GCs and play an important role in GC proliferation and development.

Baarends *et al.* found that mouse oocytes appeared to be *Amhr2* mRNA negative [34]. Jorgez *et al.* found that some oocytes in mice have positive β-gal activity via β-galactosidase activity to display *Amhr2-Cre* expression [19]. Considering that the intensity of the staining in some oocytes is not consistent with that in adjacent granulosa cells, they suggested that the apparent β-gal activity in these oocytes was unlikely to be a staining artifact [19]. Previous studies have found that Cre recombinase has variable efficiency and cannot completely delete the target protein in GCs when using *Amhr2cre* [20,21,28,29]. Therefore, incomplete ablation of cyclin B1 may be the main reason why only 32.4% of oocytes failed to undergo a second meiosis in GC-specific cyclin B1 knockout mice (Figure 5b). The progression of meiosis is controlled by cyclin B-CDK1 kinase activity [5,11]. The oocytes could not enter meiosis II due to failed cyclin B1-CDK1 kinase activity elevation caused by cyclin B1 deletion [11]. Therefore, cyclin B1-CDK1 kinase may be inactivated in oocytes with interphase-like nuclei from *Ccnb1* cKOmice.

Granulosa cells transmit some indispensable signals and metabolites required for oocyte growth and maturation to oocytes by gap junctions [17]. Consistent with this, cyclin B1 deletion of GCs could affect the meiotic progression of oocytes. The oocytes with interphase-like nuclei were easily misidentified as zygotes when collecting them from the oviduct, which is one of the reasons for the decreased rate of embryos during *in vitro* culture. Additionally, cells cannot divide without Cyclin B1 in mouse embryos [9]. Successful mitosis requires that cyclin B1:CDK1 kinase activity remains high until chromosomes are correctly aligned on the mitotic spindle [35,36]. Given that cyclin B1–*null* embryos arrest at the four-cell stage in G2 phase after DNA replication in mice [9], maternal *Ccnb1* mRNA may play an important role in embryo development before the four-cell stage. It is possible that the quality and developmental ability of embryos become poor if an inadequate reserve of *Ccnb1* mRNA from oocytes occurs.

In conclusion, Cyclin B1 in GCs is dispensable for folliculogenesis. However, GC-specific Cyclin B1 knockout mice are subfertile. Oocytes with interphase-like nuclei miscounted as zygotes is one of the reasons for the decreased rate of embryos in *Ccnb1* cKO mice. This study provides a crucial complement for the role of cyclin B1 in the reproductive activity of female mice.

Data availability statement

The data used to support the findings of this study are included within the article.

Disclosure statement

No potential conflict of interest was reported by the author(s).

Funding

This work was supported by the National Natural Science Foundation of China (82001615) and Nantong Science and Technology Project (Grant Nantong Science and Technology Bureau JC2019025).

References

[1] Murray AW, Kirschner MW. Cyclin synthesis drives the early embryonic cell cycle. Nature. 1989;339:275–280.
[2] Lohka MJ, Hayes MK, Maller JL. Purification of maturation-promoting factor, an intracellular regulator of early mitotic events. Proc Natl Acad Sci USA. 1988;85:3009–3013.
[3] Dorée M, Hunt T. From Cdc2 to Cdk1: when did the cell cycle kinase join its cyclin partner?. J Cell Sci. 2002;115:2461–2464.
[4] Polański Z, Homer H, Kubiak JZ. Cyclin b in mouse oocytes and embryos: importance for human reproduction and aneuploidy. Mouse Develop. 2012: 69–91.
[5] Satyanarayana A, Kaldis P. Mammalian cell-cycle regulation: several cdks, numerous cyclins and diverse compensatory mechanisms. Oncogene. 2009;28:2925–2939.
[6] Gavet O, Pines J. Progressive activation of cyclinb1-Cdk1 coordinates entry to mitosis. Dev Cell. 2010;18:533–543.

[7] Gavet O, Pines J. Activation of cyclin b1–Cdk1 synchronizes events in the nucleus and the cytoplasm at mitosis. J Cell Biol. 2010;189:247–259.
[8] Brandeis M, Rosewell I, Carrington M, et al. Cyclin B2-null mice develop normally and are fertile whereas cyclin B1-null mice die in utero. Proc Natl Acad Sci USA. 1998;95:4344–4349.
[9] Strauss B, Harrison A, Coelho PA, et al. Cyclin B1 is essential for mitosis in mouse embryos, and its nuclear export sets the time for mitosis. J Cell Biol. 2018;217:179–193.
[10] Tang J-X, Li J, Cheng J-M, et al. Requirement for CCNB1 in mouse spermatogenesis. Cell Death Dis. 2017;8:e3142–e3142.
[11] Li J, Tang J-X, Cheng J-M, et al. Cyclin B2 can compensate for cyclin B1 in oocyte meiosis I. J Cell Biol. 2018;217:3901–3911.
[12] Herbert M, Levasseur M, Homer H, et al. Homologue disjunction in mouse oocytes requires proteolysis of securin and cyclin b1. Nat Cell Biol. 2003;5:1023–1025.
[13] Buonomo SB, Clyne RK, Fuchs J, et al. Disjunction of homologous chromosomes in meiosis I depends on proteolytic cleavage of the meiotic cohesin Rec8 by separin. Cell. 2000;103:387–398.
[14] Kudo NR, Wassmann K, Anger M, et al. Resolution of chiasmata in oocytes requires separase-mediated proteolysis. Cell. 2006;126:135–146.
[15] Holland AJ, Taylor SS. Cyclin-B1-mediated inhibition of excess separase is required for timely chromosome disjunction. J Cell Sci. 2006;119:3325–3336.
[16] Li J, Ouyang Y-C, Zhang C-H, et al. The cyclin b2/CDK1 complex inhibits separase activity in mouse oocyte meiosis I. Development. 2019;146:dev182519.
[17] Voronina E, Lovasco LA, Gyuris A, et al. Ovarian granulosa cell survival and proliferation requires the gonad-selective TFIID subunit TAF4b. Dev Biol. 2007;303:715–726.
[18] Cheng J, Li YC, Zhang Y, et al. Conditional deletion of wntless in granulosa cells causes impaired corpora lutea formation and subfertility. Aging (Albany NY). 2021;13:1001.
[19] Jorgez CJ, Klysik M, Jamin SP, et al. Granulosa cell-specific inactivation of follistatin causes female fertility defects. Mol Endocrinol. 2004;18:953–967.
[20] Li Q, Pangas SA, Jorgez CJ, et al. Redundant roles of SMAD2 and SMAD3 in ovarian granulosa cells in vivo. Mol Cell Biol. 2008;28:7001–7011.
[21] Pangas SA, Jorgez CJ, Tran M, et al. Intraovarian activins are required for female fertility. Mol Endocrinol. 2007;21:2458–2471.
[22] Fu X, Cheng J, Hou Y, et al. The association between the oocyte pool and aneuploidy: a comparative study of the reproductive potential of young and aged mice. J Assist Reprod Genet. 2014;31:323–331.
[23] Cheng J-M, Li J, Tang J-X, et al. Elevated intracellular pH appears in aged oocytes and causes oocyte aneuploidy associated with the loss of cohesion in mice. Cell Cycle. 2016;15:2454–2463.
[24] Peltoketo H, Strauss L, Karjalainen R, et al. Female mice expressing constitutively active mutants of FSH receptor present with a phenotype of premature follicle depletion and estrogen excess. Endocrinology. 2010;151:1872–1883.
[25] Hong X, Luense LJ, McGinnis LK, et al. Dicer1 is essential for female fertility and normal development of the female reproductive system. Endocrinology. 2008;149:6207–6212.
[26] Boerboom D, White LD, Dalle S, et al. Dominant-stable beta-catenin expression causes cell fate alterations and wnt signaling antagonist expression in a murine granulosa cell tumor model. Cancer Res. 2006;66:1964–1973.
[27] Hernandez Gifford JA, Hunzicker-Dunn ME, Nilson JH. Conditional deletion of beta-catenin mediated by Amhr2cre in mice causes female infertility. Biol Reprod. 2009;80:1282–1292.
[28] Boerboom D, Paquet M, Hsieh M, et al. Misregulated Wnt/β-catenin signaling leads to ovarian granulosa cell tumor development. Cancer Res. 2005;65:9206–9215.
[29] Pangas SA, Li XH, Umans L, et al. Conditional deletion of Smad1 and Smad5 in somatic cells of male and female gonads leads to metastatic tumor development in mice. Mol Cell Biol. 2008;28:248–257.
[30] Li J, Tang JX, Cheng JM, et al. Cyclin b2 can compensate for cyclin B1 in oocyte meiosis I. J Cell Biol. 2018;217:3901–3911.
[31] Cheng J-M, Li J, Tang J-X, et al. Merotelic kinetochore attachment in oocyte meiosis II causes sister chromatids segregation errors in aged mice. Cell Cycle. 2017;16:1404–1413.
[32] Bellanger S, De Gramont A, Sobczak-Thepot J. cyclin b2 suppresses mitotic failure and DNA re-replication in human somatic cells knocked down for both cyclins B1 and B2. Oncogene. 2007;26:7175–7184.
[33] Soni DV, Sramkoski RM, Lam M, et al. cyclin B1 is rate limiting but not essential for mitotic entry and progression in mammalian somatic cells. Cell Cycle. 2008;7:1285–1300.
[34] Baarends WM, Uilenbroek JT, Kramer P, et al. Anti-müllerian hormone and anti-müllerian hormone type II receptor messenger ribonucleic acid expression in rat ovaries during postnatal development, the estrous cycle, and gonadotropin-induced follicle growth. Endocrinology. 1995;136:4951–4962.
[35] Hayward D, Alfonso-Pérez T, Gruneberg U. Orchestration of the spindle assembly checkpoint by CDK1-cyclin B1. FEBS Lett. 2019;593:2889–2907.
[36] Levasseur MD, Thomas C, Davies OR, et al. Aneuploidy in oocytes is prevented by sustained CDK1 activity through degron masking in cyclin B1. Dev Cell. 2019;48:672–684. e675.